

# Influence of interfacial adhesion on the mechanical response of magneto-rheological elastomers at high strain

T. Pössinger · C. Bolzmacher · L. Bodelot ·  
N. Triantafyllidis

Received: 2 August 2013 / Accepted: 7 December 2013 / Published online: 19 December 2013  
© Springer-Verlag Berlin Heidelberg 2013

**Abstract** This work investigates the interfacial adhesion between the iron fillers and the silicone matrix in magneto-rheological elastomers (MREs) at high strain. Carbonyl iron powder, composed of mechanically soft spherical particles with a median size of 3.5  $\mu\text{m}$  and a volume fraction of 3.5 and 30 %, was mixed in a soft silicone matrix; the compound was then degassed and cured under temperature. The presence of a homogeneous magnetic field of 0.3 T during the curing process allowed the formation of particle chains. Tensile tests of these samples were conducted under scanning electron microscope to simulate and observe interfacial debonding between the two phases. To improve interfacial adhesion, a silane primer was applied to the iron particles, following two different procedures, before the mixing and crosslinking process, thus giving two additional types of samples for each volume fraction. In-situ scanning electron microscope measurements during tensile tests showed that a more elaborated particle–matrix interface was obtained with the primer additive. Furthermore, the structural response of the different types of samples were compared in tensile testing lengthwise to the particle alignment with engineering strains up to 150 %. An enhanced adhesion of the iron fillers to the silicone matrix resulting in a largely increased stiffness at high strain could be observed with the application of the primer. It was observed that the effect of the primer on the debonding of the particles from the silicone matrix has an impact on the

macroscopic behavior of the composite only after 80 % deformation in the case of the 30 % volume fraction MRE.

## 1 Introduction

Materials whose rheological properties can be varied by the application of magnetic fields belong to the specific class of smart materials because they can respond rapidly and reversibly to changes in their environment. As a branch of this kind of materials, so-called magneto-rheological elastomers (MREs) are typically composed of micron-sized magnetic particles dispersed in an elastomeric matrix. When a magnetic field is applied to the elastomer composite during crosslinking, particle chain structures form and remain locked in place upon final curing, thus imparting anisotropic properties to a viscoelastic material (Carlson and Jolly 2000; Kallio 2005; Li and Zhang 2008). Not only do MREs alter their viscoelastic properties in response to an external magnetic field but they also can undergo very high deformation states. While the former effect is mainly exploited in variable and controllable stiffness devices (Carlson and Jolly 2000; Li and Zhang 2008), the latter may be of interest in haptic devices such as a tactile interface (Vidal-Verdu and Hafez 2007). Indeed, a large out-of-plane deformation can be introduced in response to a spatially localized magnetic field. Using a matrix of solenoids or permanent magnets placed underneath a soft MRE surface, patterns can be displayed on the surface (see Fig. 1) as already achieved with magneto-rheological fluids (Bolzmacher et al. 2011; Jansen et al. 2010; Lee and Jang 2011; Sgambelluri et al. 2008).

It is well known that the macroscopic behavior of filled polymers is affected by polymer-filler and filler–filler interactions. Phenomena like the influence of the strain

T. Pössinger (✉) · C. Bolzmacher  
CEA LIST Sensorial and Ambient Interfaces Laboratory,  
91191 Gif-sur-Yvette CEDEX, France  
e-mail: tobias.possinger@cea.fr

L. Bodelot · N. Triantafyllidis  
Ecole Polytechnique, Laboratoire de Mécanique des Solides,  
Route de Saclay, 91128 Palaiseau, France

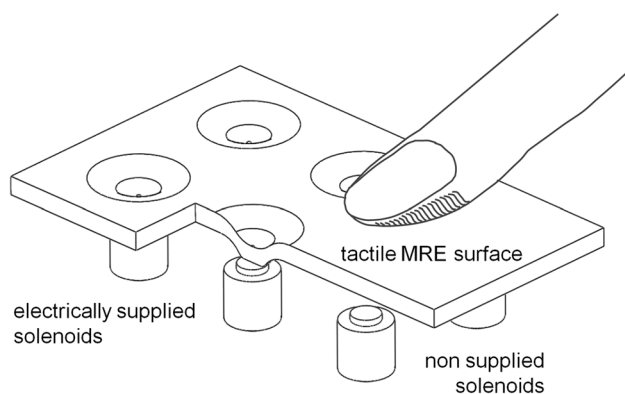


**Fig. 1** Schematics of a tactile MRE surface with patterns created by a solenoid matrix placed underneath

amplitude on the stiffness at small deformations (so-called “Payne effect”; Böhm 2001; Payne 1962) or on the amount of softening between first and subsequent load cycles (so-called “Mullins effect”; Diani et al. 2009; Dorfmann and Ogden 2004; Miehe and Keck 2000; Mullins and Tobin 1957) can be observed experimentally in filled polymers and can be linked to changes in the microstructure. Size, shape, distribution and volume fraction of the filler particles are therefore important parameters (Leblanc 2002; Ramier 2004). For polymers containing rigid fillers with small aspect ratios, such as spherical particles, the stiffness is mainly increased with higher particle volume fraction (Fu et al. 2008). Moreover, filler networks such as particle chain structures and agglomerates further increase the stiffness of the composite material due to the fact that rubber gets entrapped in the network. Hence, this leads to an increase of the effective filler volume, as long as the filler network is not broken down (Wang 1999; Yatsuyanagi et al. 2001).

Another important aspect influencing the strength of the composite material is the interfacial adhesion between the filler particles and the matrix (Dekkers and Heikens 1983; Fu et al. 2008). Indeed, at a critical stress level, debonding acts as a distinct failure phenomenon in a polymer containing rigid inclusions due to stress concentrations at a weak particle–matrix interface (Creton et al. 2001; Gent and Park 1984). In order to modify the particle–matrix interactions and more precisely to improve the interfacial adhesion, the modification of the surface properties of the system has been suggested (Léger and Creton 2008; Zhang et al. 2007) and different kinds of silane coupling agents and compatibilizer have been used in MREs (Coquelle and Bossis 2006; Coquelle et al. 2006; Fan et al. 2010; Wang et al. 2006). A silane coupling agent or primer typically consists of two different reactive groups, one compatible with the filler particles and the other one with the elastomer matrix. Applied in a thin, theoretically monomolecular

layer, the primer serves as an adhesion promoter between the two nonbonding surfaces (Habenicht 2006). Some studies showed the improved bond strength between many primed metallic surfaces and addition-cured silicon elastomers (Peignot and Rhodes 2004). Hence, the phenomenon of interfacial adhesion appears to be a key property for the behavior of filler-soft elastomer composites. Indeed, to preserve the magneto-mechanical coupling and the related effects, it is of interest that the filler particles in the MREs remain locked in place under high deformation states. But so far, interfacial adhesion at high tensile deformations in soft MREs has rarely been investigated in detail. To the authors’ knowledge there is no literature on the level of deformation to which the mechanical adhesion can be preserved.

In the perspective of developing a persistent tactile MRE surface with reversible and large out-of-plane deformation, this work investigates the interfacial adhesion between the iron fillers and the silicone matrix at high strain. Therefore, different MRE samples are prepared by modifying the surface of carbonyl iron particles (CIP) via silane primer treatment according to two procedures, prior to compounding. These samples are then compared to a sample without particle treatment both under scanning electron microscope (SEM) and during mechanical testing. First, we describe the experimental procedures for the sample preparation, the SEM observation and the mechanical testing (Sect. 2). The experimental results are presented in Sect. 3 and discussed in Sect. 4.

## 2 Experimental

### 2.1 Materials

The very soft and stretchable silicone elastomer Ecoflex 0020 from Smooth-On Inc., USA, was chosen as the matrix material to facilitate high deformations under a small magnetic field for a possible application in a tactile MRE interface. This elastomer is a two-part addition cured platinum-catalyzed system (RTV-2). The obtained silicone has a Shore hardness of 00–20, an elongation at break of 845 %, a density of 1.07 g/cm<sup>3</sup> and a pot life time of 30 min according to the manufacturer.

Mechanically and magnetically soft spherical carbonyl iron powder CIP SM with a median particle size of 3.5 μm and a density of 7.5 g/cm<sup>3</sup> from BASF, Germany, was used as the filler material.

To improve adhesion between the silicone elastomer and the iron particles, the clear 1200 OS Primer from Dow Corning, USA, was used. The 5 % non-volatile active content of this silane based primer is diluted in volatile siloxanes as purchased.

**Table 1** Volume fractions and particle pretreatment for the different types of samples prepared in this study

	Pure silicone	Untreated MRE	Spray-coated MRE	Primer stirred MRE
Silicone elastomer (%)	100	96.5	70	96.5
CIP volume fraction (%)	0	3.5	30	3.5
Silane primer treatment of CIP	n/a	None	Particles spray-coated by dilution	Particles stirred in dilution

### 2.2 Samples preparation

A pure silicone elastomer and different MRE samples were prepared, modifying or not, the surface of CIP by silane primer treatment of the particles prior to compounding. The silane primer dilution was applied according to two procedures: either by spray-coating the particles with it or by stirring the particles in it. In order to observe the MREs’ microstructures clearly under the microscope, a low particle volume fraction of 3.5 % was considered first. To investigate the case of MREs used in engineering applications, another series of samples with a high volume fraction of 30 % was prepared. All the MRE samples were cured in the presence of a magnetic field of 0.3 T. The different types of samples used in this work are summarized in Table 1 and details regarding their fabrication are given in the following sections.

#### 2.2.1 Pure silicone

A pure silicone material sample without filler was prepared. The polymer (Part A) and the crosslinker (Part B) were dispensed in a 1:1 weight ratio and thoroughly mixed for 3 min by a mechanical stirring machine at 400 rpm. Then, the mixed material was degassed at 1 mbar for 8 min to eliminate any entrapped air and poured by hand in a copper-Teflon mold presented in Fig. 2. The curing was accelerated by heating the mold up to 100 °C for 30 min and then cooling it back to room temperature (see Fig. 3). This was achieved by equipping the mold with a thermoelectric power generation system made of Peltier elements coupled via a heatsink to a fan (see Fig. 2). The samples were finally demolded, having a volume of  $24 \times 24 \times 4 \text{ mm}^3$  (see also Fig. 6).

#### 2.2.2 Untreated MRE

A series of MRE samples without silane particle treatment was prepared by adding 40 % in weight of silicone (Part A), 40 % in weight of crosslinker (Part B) and 20 % in weight of iron particles. This weight fraction of 20 % corresponds to a volume fraction of about 3.5 % of carbonyl iron particles. Another series of MRE samples with a particle volume fraction of 30 % was prepared in the same way. The material was then mixed, degassed and cured as the pure silicone samples except for the mold being placed under

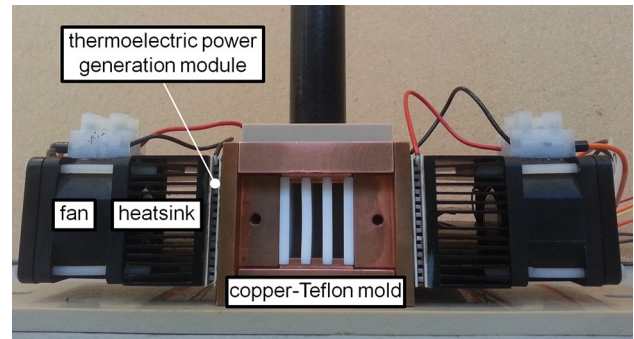


**Fig. 2** Copper-Teflon mold and thermoelectric power generation system made of Peltier elements coupled via a heatsink to a fan

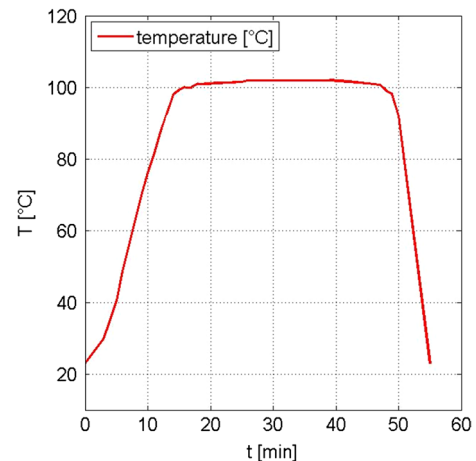


**Fig. 3** Curing schedule of the samples as a function of temperature over time

a constant magnetic field of 0.3 T. The magnetic field was applied with a coil-permanent magnet device presented in Fig. 4 and caused the particles to align in chain-like structures in the direction of the field. A finite element simulation with the Finite Element Method Magnetics (FEMM) software shows that the field is homogeneous in the zone where the samples are placed (see Fig. 5).

#### 2.2.3 Spray-coated MRE

A series of MRE samples was prepared by first dispersing the particles in a plastic container and spraying them with the

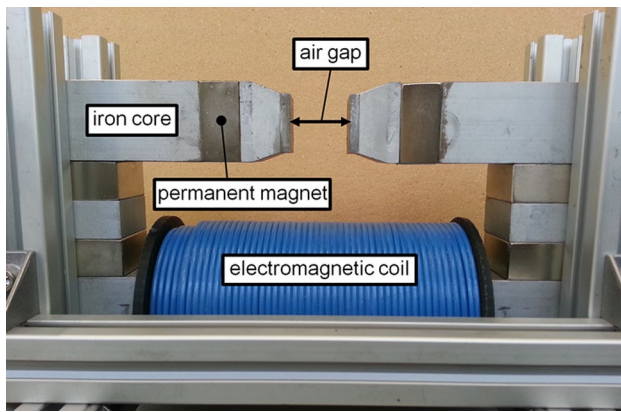


**Fig. 4** Coil-permanent magnet device to create a constant magnetic field of 0.3 T guided by an iron core through the air gap

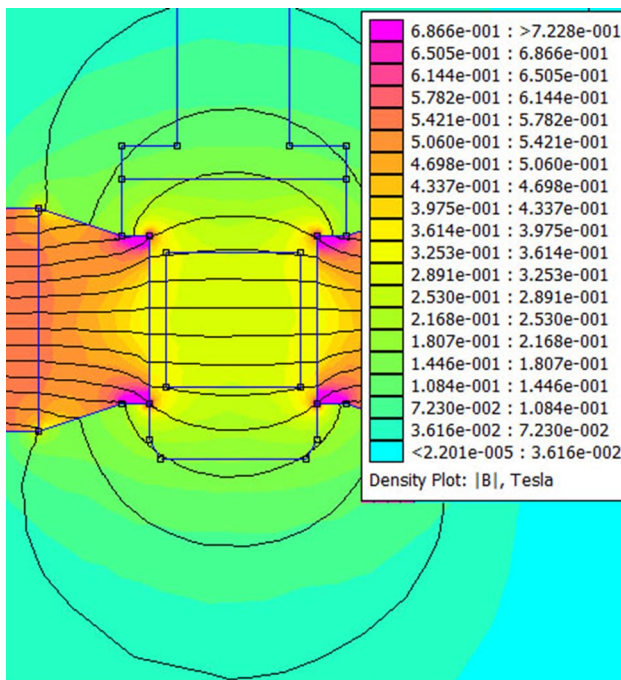


**Fig. 5** FEM simulation showing the homogeneity of the magnetic flux inside the air gap

primer using an air brush while shaking the container. After 45 min of air drying, the spray-coated particles were mixed into the silicone so that the volume fraction of the particles was either 3.5 or 30 %. The compound was finally degassed and cured under field identically to the untreated MRE samples.

#### 2.2.4 Primer stirred MRE

Another series of MRE samples was prepared by directly stirring the iron particles in the silane primer dilution. After the stirring process, the particle-primer-mix was widely

dispersed on a Teflon plate, rinsed out with Ethanol and air dried for 45 min. Mixing, degassing and curing under field were then carried out, as described in the previous sections, for particle volume fractions of 3.5 and 30 %.

### 2.3 Scanning electron microscopy

To evaluate the effect of primer application and the subsequent interfacial adhesion between the iron fillers and the silicone matrix, both the untreated and primer treated particles, as well as the three corresponding types of MRE samples described in Sect. 2.2, were analyzed by using an environmental Quanta 600 FEG scanning electron microscope (SEM). A beam voltage of 5 kV and an Everhart–Thornley detector were used in high-vacuum mode for the investigation of the untreated and primer treated particles. However, the investigation of the MRE samples was performed in low-vacuum mode with a chamber pressure of 130 Pa and environmental water vapor in order to limit charge phenomena during the imaging of the low conductivity material. In this case, a beam voltage of 10 kV and a back-scattered electron detector were used. For the observation of the particle chains, the samples were cut parallel to the chain orientation using a scalpel along the surface highlighted in Fig. 6. An in situ traction stage inside the SEM was used to pull on the MRE samples up to 140 % strain parallel to the particle chains, thus allowing us to image the composites' microstructure at high deformation states.

### 2.4 Mechanical measurements

The structural response of the different MRE samples and the pure silicone elastomer was studied in traction tests at

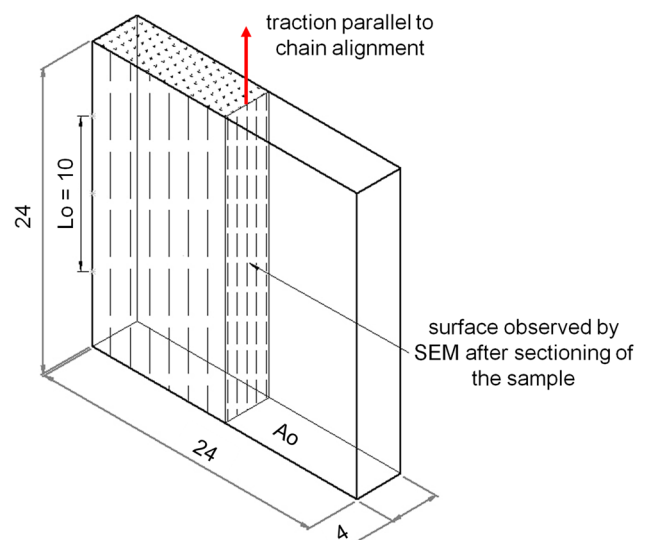


**Fig. 6** Sample geometry (dimensions in mm) for SEM observation and mechanical measurements

room temperature (23 °C). Each sample was maintained by mechanical grips separated by an initial distance  $L_0$  of 10 mm. The elongation of the sample was imposed, with an accuracy of <math> < 50 \mu\text{m}</math>, by the displacement of the motors to which the grips were attached. The tensile force was measured by a 10 N universal load cell (Althen ALF328) with an accuracy of <math> < 50 \text{ mN}</math>. The nominal stress was calculated as the ratio of the axial force to the undeformed cross-sectional area  $A_0$  of the sample that is  $24 \times 4 \text{ mm}^2$  (see Fig. 6). The nominal strain was calculated as the ratio of the current elongation to the initial length. All samples were subjected to a sinusoidal cyclic loading between the unstrained state and a maximum strain of 150 % at a strain rate of  $0.02 \text{ s}^{-1}$ .

### 3 Results

#### 3.1 Macroscopic preliminary investigations

Preliminary macroscopic investigations were conducted at the beginning of this study to illustrate the phenomenon of interfacial debonding of rigid spherical particles from the soft silicone matrix (Fig. 7). Spheres of steel, as those in ball bearings, with a diameter of 1.5 mm were molded in the Ecoflex 0020 silicone elastomer and subjected to traction up to nominal tensile strain of 40 %. It can be observed

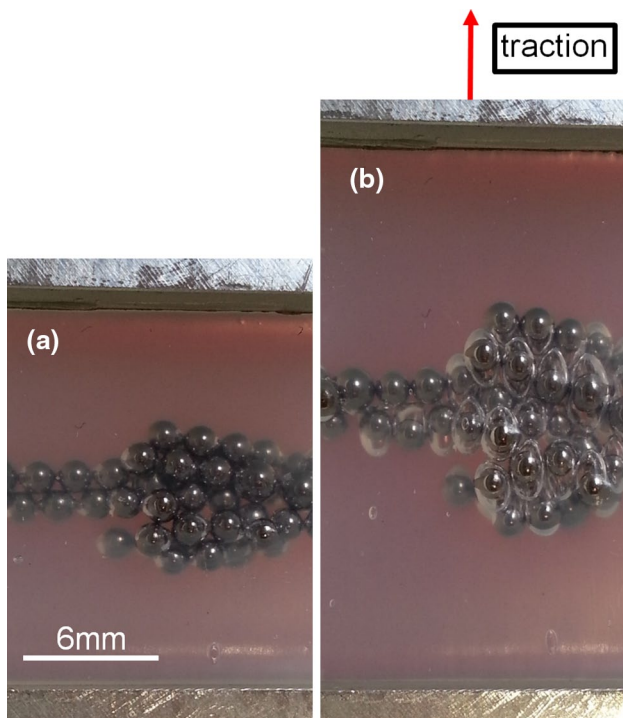


**Fig. 7** Preliminary macroscopic test: **a** 1.5 mm steel spheres cast in the silicone matrix at the unstrained state; **b** debonding between spheres and silicone matrix under traction at 40 % nominal strain

that there is a strong debonding between the spheres and the elastomeric matrix, starting already at small strain and being more pronounced around large particle agglomerates. It is worth mentioning that this test with large spheres was for an illustrative purpose only. As a matter of fact, very important parameters for the adhesion between the filler particles and the rubber are the particle size, the surface quality and the material.

Further investigations focused on the strength of the bond between the silicone matrix material to be employed and an iron plate that was either untreated or treated with primer. Two pure iron plates (Telar 57) were polished to an average surface finish of  $0.125 \mu\text{m}$  to imitate the surface roughness of the CIP. The silicone elastomer was then cast with a cross-section of  $18 \times 18 \text{ mm}^2$  between the two plates placed at an initial distance of 3 mm. During traction tests, the debonding of the silicone from the untreated and primer treated (brushing with silane primer and air drying) iron plates was studied (see Fig. 8). The nominal stress–strain curves presented in Fig. 9 depict that the adhesion of

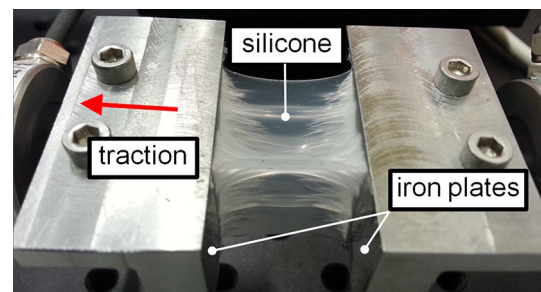


**Fig. 8** Image of the traction test of the silicone cast between two primer treated iron plates in the deformed state

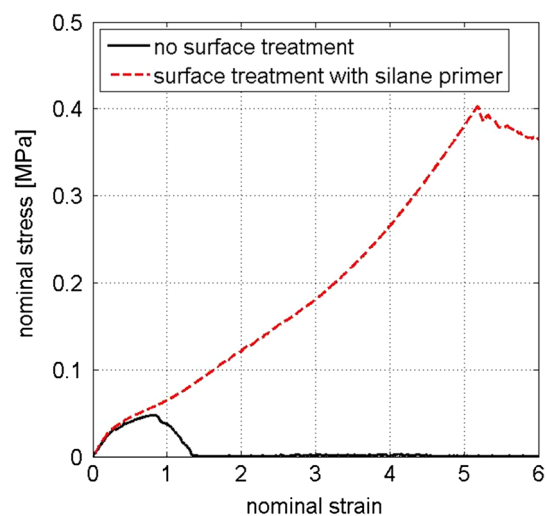


**Fig. 9** Nominal stress–strain curves illustrating the improved adhesion of the silicone elastomer to the primer treated iron surface compared to the untreated surface

the silicone to the primer treated iron surface is increased compared to the untreated surface. As a matter of fact, the silicone elastomer starts to debond from the untreated iron surface by slowly peeling off at a strain of 80 % while the silicone elastomer does not start to debond until 520 % in the case of the primer treated iron surface.

## 3.2 Scanning electron microscopy

### 3.2.1 Particles alone

To evaluate the effect of the primer, both the untreated and the primer treated particles were investigated by SEM and the corresponding images are confronted in Fig. 10. While the untreated (Fig. 10a) and the spray-coated (Fig. 10b) particles are loosely assembled, the primer stirred particles (Fig. 10c) are stuck together in irregular aggregates by the non-volatile primer content. Homogeneously covered particles or particle aggregates can actually be found among the spray-coated particles (Fig. 10e). In contrast, the majority of the primer stirred particles are largely covered, though rather unevenly, by the silane primer treatment as shown in Fig. 10f.

### 3.2.2 Global observation of MRE

The SEM micrographs of the 3.5 % particle volume fraction MREs with untreated, spray-coated and primer stirred

particles are first taken without any in situ traction to show the influence of the primer treatment on chain alignment. They are presented in Fig. 11 where the dark silicone in the back highlights the iron particles appearing as white spots. There is no remarkable difference in chain alignment between the untreated (Fig. 11a) and the spray-coated (Fig. 11b) samples. In both cases, the particles cured under a magnetic field of 0.3 T are aligned in thin disconnected chains spaced with small distances. In contrast, particle chains in the primer stirred MRE (Fig. 11c) create thick columns of irregular particle agglomerates separated by larger distances.

The 30 % particle volume fraction MREs with untreated, spray-coated and primer stirred particles were also globally observed under SEM without any in situ traction (Fig. 12). The aligned particle chain structures (due to the application of a magnetic field of 0.3 T during fabrication) are not as clearly visible as for the 3.5 % volume fraction MREs. For all samples, there are very small distances between the irregular particle chains because of the high particle content. Nevertheless, the samples behave identically as the ones with lower particle volume fraction shown in Fig. 11. Again, no remarkable differences can be seen between the untreated (Fig. 12a) and the spray-coated (Fig. 12b) samples. However, in the case of the primer stirred MRE (Fig. 12c), irregular particle agglomerates are embedded in surrounding evenly distributed chain structures.

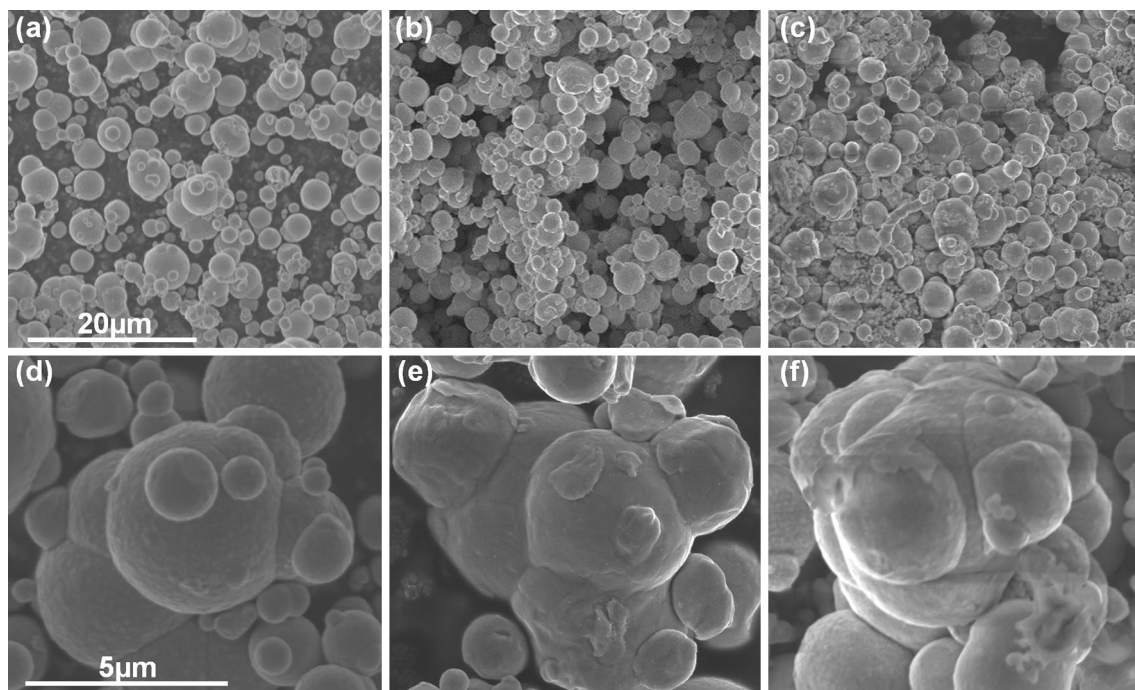


**Fig. 10** SEM micrographs (1,500 $\times$ ) of the carbonyl iron particles with a median particle size of 3.5  $\mu\text{m}$ : **a** untreated particles, **b** spray-coated particles, and **c** primer stirred particles; SEM micrographs

(6,000 $\times$ ) of, **d** untreated particles, **e** spray-coated particles, and **f** primer stirred particles

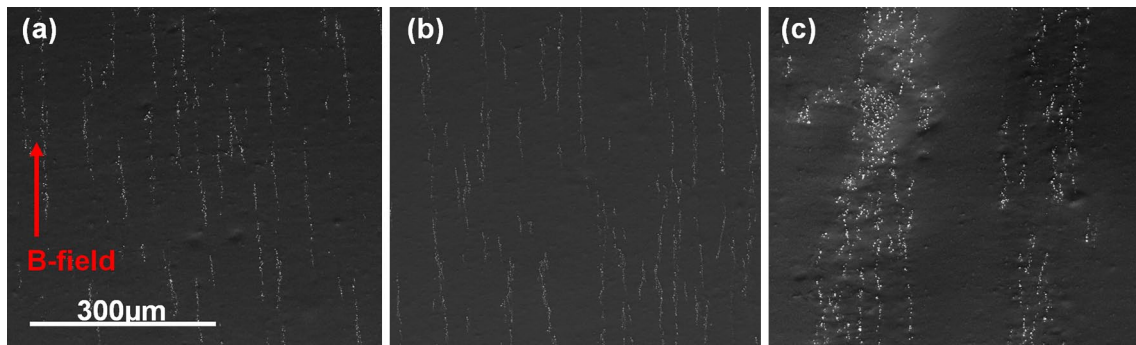


**Fig. 11** SEM micrographs (200×) of particle chain alignment in MRE samples with a particle volume fraction of 3.5 %: **a** untreated MRE, **b** spray-coated MRE, and **c** primer stirred MRE. The *arrow* indicates the direction of the magnetic field during curing

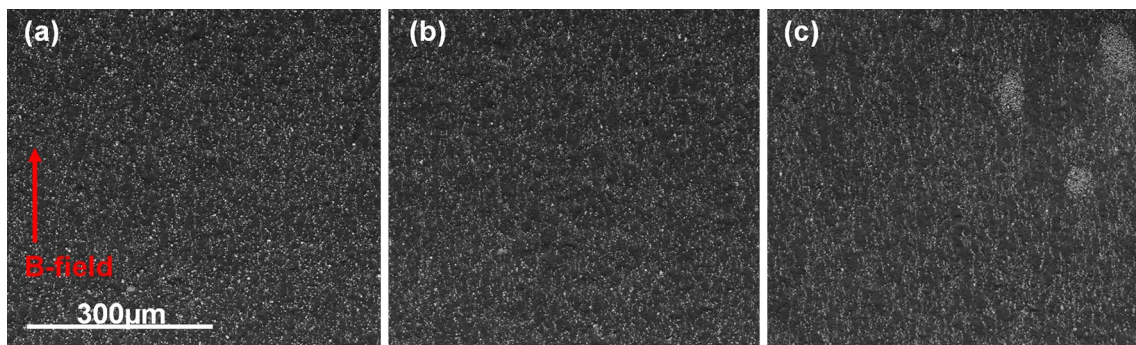


**Fig. 12** SEM micrographs (200×) of particle chain alignment in MRE samples with a particle volume fraction of 30 %: **a** untreated MRE, **b** spray-coated MRE, and **c** primer stirred MRE. The *arrow* indicates the direction of the magnetic field during curing

### 3.2.3 Local observation of MRE

To study the interfacial adhesion between the iron fillers and the silicone matrix at high deformation states, the longitudinal sections (see Fig. 6) of the different MRE samples were observed by SEM at a nominal strain of 140 % applied with an in situ traction device. While imaging, irradiation by the 10 kV electron-beam caused a local deterioration of the matrix. The surface of the silicone matrix undulates at the region of irradiation and next to it as depicted in Fig. 13. This phenomenon was also observed for MREs consisting of other silicone matrix materials. Besides, in electron-beam lithography this effect of deterioration of the material by irradiation is used to etch off polymers from substrates (Geissler and Xia 2004). The presence of fillers like particles, especially large particle agglomerates, already partly set free from the matrix because of the initial scalpel cut, leads to the formation of pores in the damaged elastomeric matrix when loaded. The fact that the opening of the matrix was not due to mechanical stresses could be proven by observing a MRE sample that was previously cycled 12 times up to 150 % strain outside of the SEM. This sample was then placed back in the

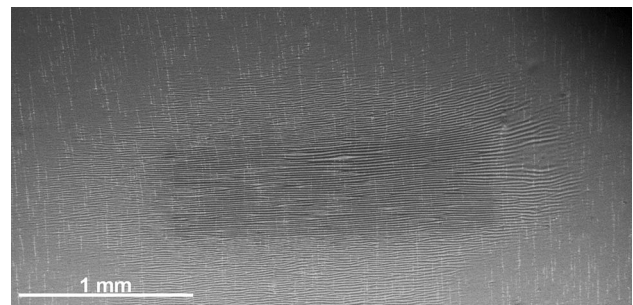


**Fig. 13** SEM micrograph (25×) showing the deterioration of the silicone matrix due to the 10 kV electron-beam: the initially flat surface now exhibits undulation

SEM, loaded up to a nominal strain of 140 % and imaged while paying attention to minimize the focus time: it did not show any pore opening.

The electron-beam induced deterioration of the material and the subsequent formation of pores under loading conditions allowed us to further investigate the interfacial adhesion between the iron fillers and the silicone matrix at a local scale. SEM micrographs of the samples

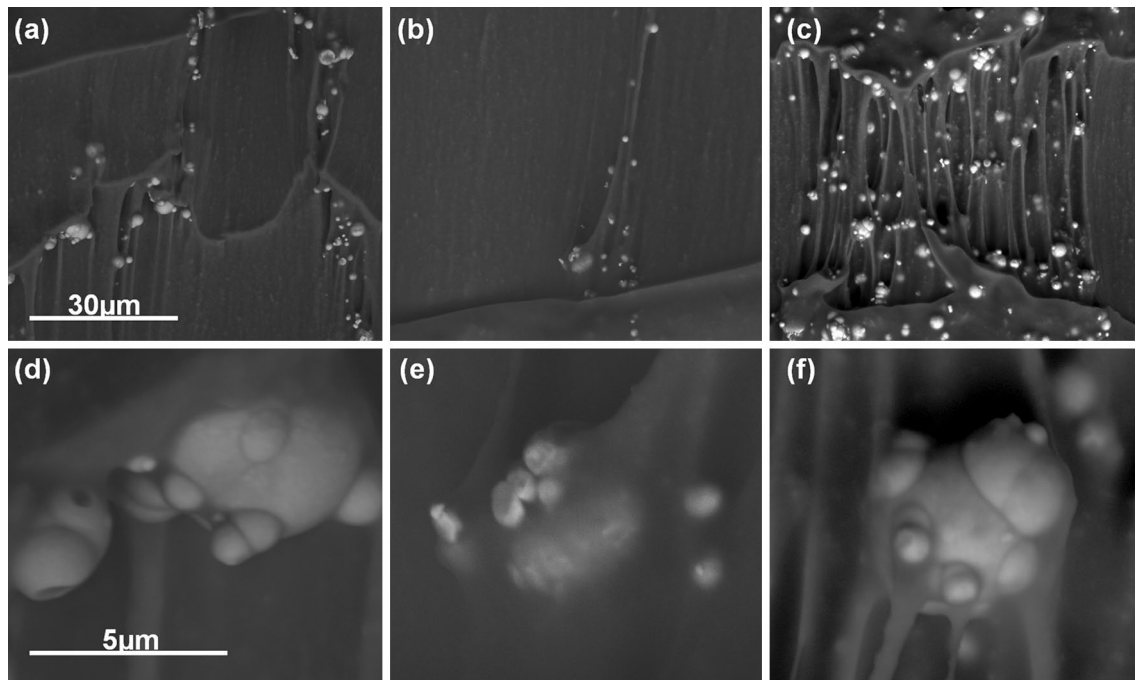


**Fig. 14** SEM micrographs (1,500 $\times$ ) of the interfacial adhesion between the iron fillers and the silicone matrix at a strain of 140 % in MRE samples with a particle volume fraction of 3.5 %: **a** untreated

MRE, **b** spray-coated MRE, and **c** primer stirred MRE; SEM micrographs (12,000 $\times$ ) of **d** untreated MRE, **e** spray-coated MRE, and **f** primer stirred MRE

loaded at 140 % nominal strain show that the silicone matrix detaches from the particles without any remaining residues for the untreated MRE (Fig. 14a, d). However, in the case of the spray-coated MRE, where homogeneously covered particles could be observed (Fig. 10b, e), we can detect some particles to which the matrix is still rather well attached (Fig. 14b, e). Also in the case of the primer stirred MRE (Fig. 14c, f), some of the particles show residues of bound rubber at the interfaces and the matrix still adheres to the primed surface in separate filaments. These observations are in agreement with the previous SEM images of the different particle treatments before compounding (Fig. 10).

MREs containing a 30 % particle volume fraction show the same tendencies at a local scale when the samples are loaded up to 140 % nominal strain. The silicone matrix detaches from the particles without any remaining residues for the untreated MRE (Fig. 15a, c). In the case of the spray-coated MRE, some of the particles seem again to be rather well attached to the matrix (Fig. 15b, e). And also in the case of the primer stirred MRE (Fig. 15c, f) the particles show residues of bound rubber at the interfaces, where the matrix surrounds the filler particles.

### 3.3 Mechanical measurements

To investigate the relationship between interfacial adhesion and the structural response of a sample, cyclic tests

of the different types of specimens previously observed by SEM were performed using the setup described in Sect. 2.4. The loading/unloading cycles were performed at room temperature (23 °C) in a displacement-controlled mode up to a fixed amplitude of displacement with a strain rate of 0.02 s<sup>-1</sup>. The tested samples, whose dimensions are given in Fig. 6, are initially unstrained before mechanical testing. The nominal stress–strain response of the pure silicone elastomer, the 3.5 % volume fraction MREs and the 30 % volume fraction MREs are shown in Figs. 16, 17, 18, respectively. The pure silicone elastomer (Fig. 16) shows a small difference in response between the first cycle and the following ones with only a very weak hysteresis.

In the case of the 3.5 % volume fraction MRE samples (Fig. 17), the nominal stress–strain response of the first cycle differs significantly from the following cycles. The second cycles also differ from the following ones but less significantly. There is a large stress softening after the first cycle, which diminishes with the following cycles and becomes negligible after about 6 cycles. The softening is comparable for the untreated MRE sample (Fig. 17a) and the spray-coated MRE sample (Fig. 17b) but more pronounced for the primer stirred MRE sample (Fig. 17c). After about 6 cycles, the stress–strain responses are repeatable and only exhibit a weak hysteresis for all 3.5 % volume fraction MREs.



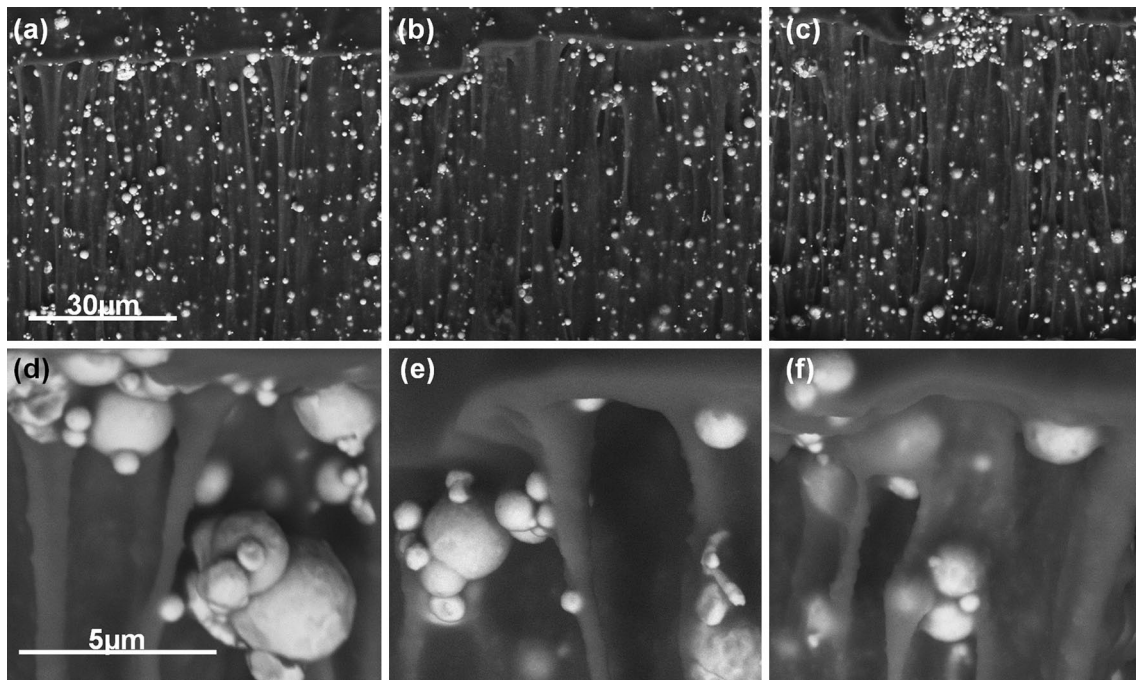


**Fig. 15** SEM micrographs (1,500×) of the interfacial adhesion between the iron fillers and the silicone matrix at a strain of 140 % in MRE samples with a particle volume fraction of 30 %: **a** untreated

MRE, **b** spray-coated MRE, and **c** primer stirred MRE; SEM micrographs (12,000×) of **d** untreated MRE, **e** spray-coated MRE, and **f** primer stirred MRE

For the 30 % volume fraction MRE samples (Fig. 18), one can again observe a significant difference in the nominal stress–strain response between the first cycle and the following ones, which stabilizes after about 6 cycles though it still slightly oscillates around a stable average value. Compared to the untreated MRE (Fig. 18a), the first cycle softening is remarkably larger for the spray-coated MRE (Fig. 18b) and even larger for the primer stirred MRE (Fig. 18c). Furthermore, for the stabilized curves, the increase in stiffness between the primer treated samples and the untreated MRE gets much more pronounced at larger strains.

Moreover, in all samples, residual stresses after the first unloading are evident. They are larger for the 30 % volume fraction MRE specimens (Fig. 18) than for the 3.5 % volume fraction MRE specimens (Fig. 17) and very small for the pure silicone specimen (Fig. 16).

#### 4 Discussion

Before analyzing the influence of the primer, the mechanical tests highlight the influence of the particle volume fraction on the stiffness and the hysteretic dissipation in particle filled elastomers. This can easily be seen on the typical S-shape response by comparing the stabilized hysteretic loop for the pure silicone, the 3.5 % volume fraction

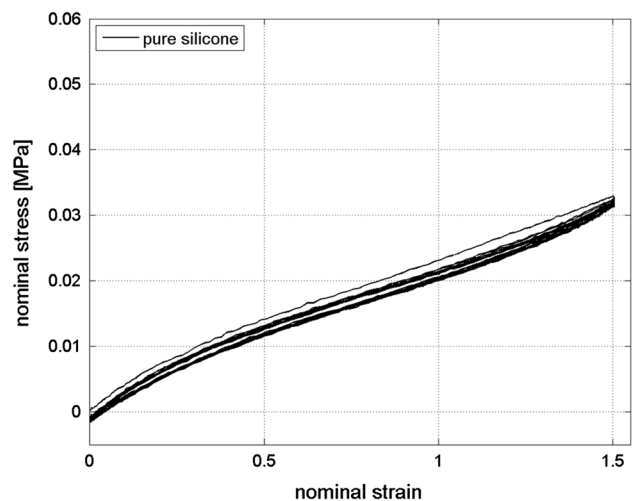


**Fig. 16** Stress-strain response of the pure silicone elastomer at a strain rate of  $0.02 \text{ s}^{-1}$

untreated MRE and the 30 % volume fraction untreated MRE (see Fig. 19). With a higher volume fraction, the stiffness of the material increases since the rigidity of the fillers is much higher than that of the matrix material. Furthermore, due to an increase of irreversible slip processes between the filler particles and a rearrangement in the polymer chain-network (Miehe and Keck 2000) the width of the hysteresis increases with higher particle volume fraction.

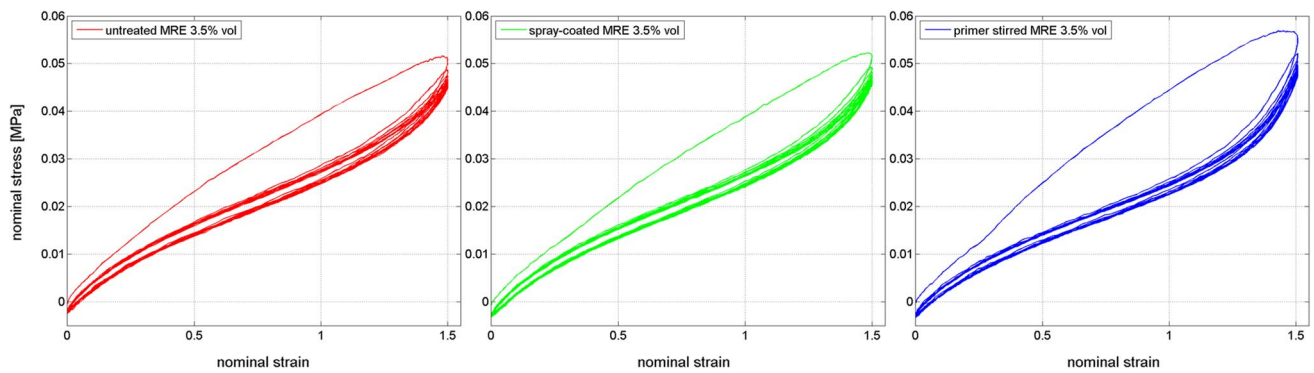


**Fig. 17** Stress-strain response of the MRE samples with a particle volume fraction of 3.5 % during cyclic loading parallel to particle alignment at a strain rate of  $0.02 \text{ s}^{-1}$ : **a** untreated MRE, **b** spray-coated MRE, and **c** primer stirred MRE

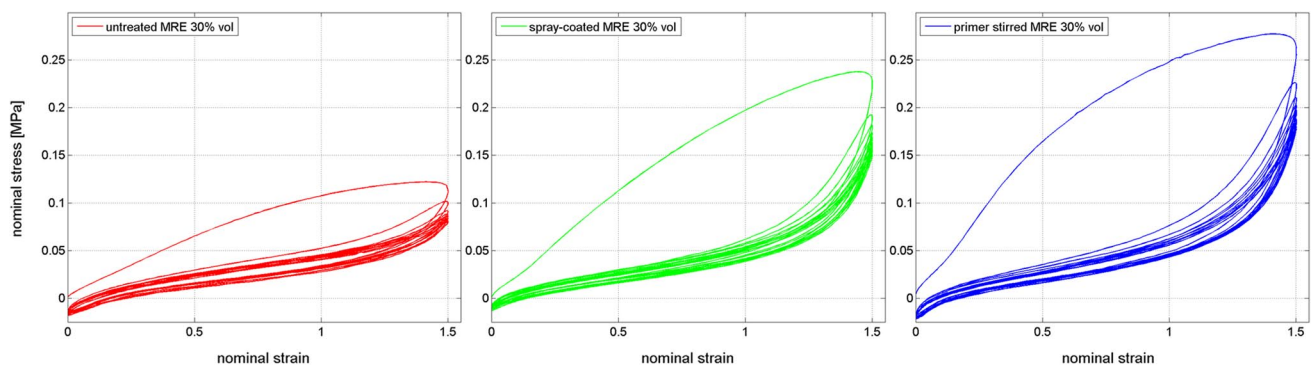


**Fig. 18** Stress-strain response of the MRE samples with a particle volume fraction of 30 % during cyclic loading parallel to particle alignment at a strain rate of  $0.02 \text{ s}^{-1}$ : **a** untreated MRE, **b** spray-coated MRE, and **c** primer stirred MRE

The application of the primer also influences the stress–strain response. Under fixed maximum deformation, the typical stress softening and large hysteretic dissipation during the first cycle increases with the particle volume fraction and is especially high for the primer treated samples. The primer application seems to create additional weak bonds between the polymer chains and the filler particles, which are destroyed during the first loading cycle.

To precisely compare the influence of the primer treatment on the stable response of the composite material, the stabilized upload curves have been studied. In the case of the 3.5 % volume fraction MREs, the addition of the primer has very little benefit (see later Fig. 21). For the 30 % volume fraction MREs (Fig. 20), there is no remarkable difference between the response of the untreated and the spray-coated MRE up to a nominal strain of 80 %. However, the 30 % volume fraction primer stirred MRE shows an increased stiffness for the stable cycle throughout the whole loading curve. It seems that the particle agglomerates further increase the stiffness due to rubber entrapped in the filler network and an increased effective filler volume (Wang 1999; Yatsuyanagi et al. 2001).

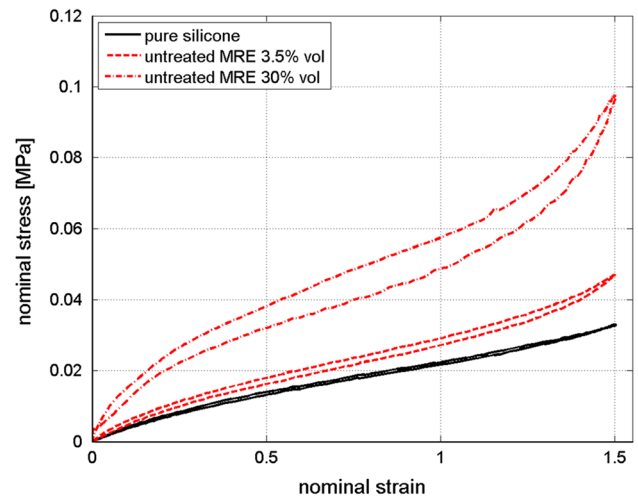


**Fig. 19** Influence of the particle volume fraction: stable cycle, once shifted to the origin, for the pure silicone, the 3.5 % volume fraction MRE and the 30 % volume fraction MRE

Hence, the application of the primer by stirring the particles in the primer dilution leads to a globally larger stiffness throughout the loading. However, this way of

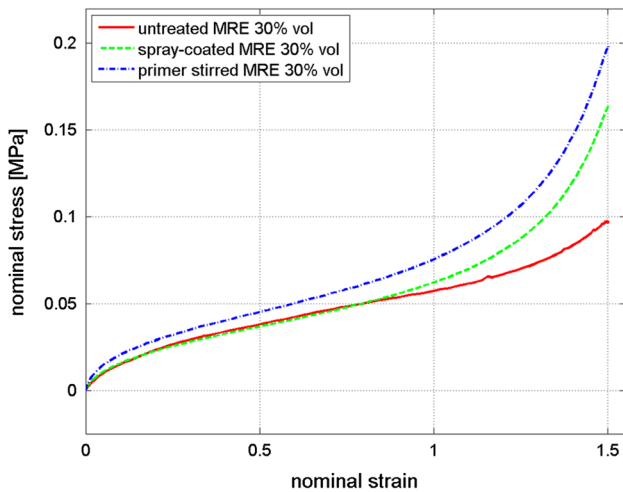


**Fig. 20** Influence of the primer treatment: stable upload curves for the 30 % volume fraction MREs

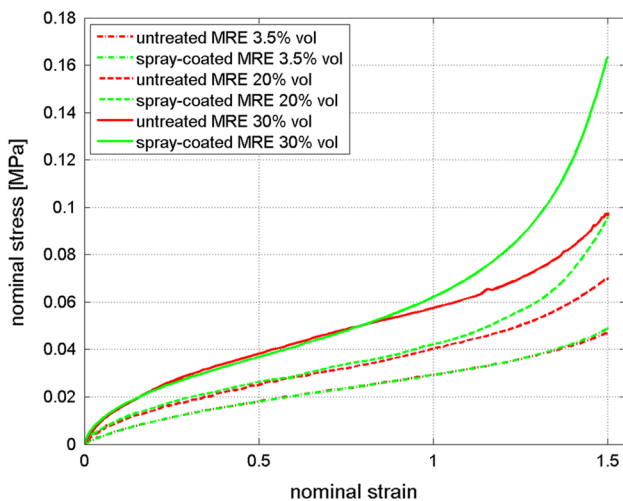


**Fig. 21** Influence of the primer treatment at high strain: stable upload curves for the spray-coated MREs compared to the untreated MREs for particle volume fractions of 3.5, 20 and 30 %

applying the primer must be discarded in our case. Indeed, it has the disadvantage of forming particle agglomerates, which is a situation that should be avoided in order to prevent field concentration during the application of a magnetic field.

Finally, we analyzed the effect of the primer, when applied by spraying, on the stiffness at high strain for different particle volume fractions (see Fig. 21). For low particle volume fractions, the application of the primer only slightly increases the ultimate stiffness. In the case of the 30 % volume fraction MREs, it could be shown that the effect of the primer was observable only beyond 80 % nominal strain. Additional tests with 20 % volume fraction MRE samples showed that for such a volume fraction, the effect of the primer was only

visible beyond 100 % nominal strain. Hence, the primer (in the spray-coated case) only enhances the MREs stiffness past a critical strain threshold that increases as the volume fraction of the particles decreases. Beyond that critical strain threshold, strong bonds due to the primer application start to stiffen the composite material and seem to prevent debonding of the particles from the matrix.

### 5 Conclusions

This work investigates the interfacial adhesion between the iron fillers and the soft silicone matrix in magneto-rheological elastomers (MREs) at high strain. For this purpose, different MRE samples with 3.5 and 30 % particle volume fraction of aligned carbonyl iron powder (CIP) were prepared with and without modification of the surface of the iron particles by the application of a silane primer following two different procedures.

Scanning electron microscope (SEM) images of simulated debonding at high strain showed that a more elaborated particle–matrix interface could be obtained with the primer additive.

The primer treatment adds another challenging process step to the fabrication. The application of the primer by stirring the particles in the primer dilution lead to an enhanced stiffness. However, it has the disadvantage of forming large particle agglomerates entrapped in the matrix, which is a situation that should be avoided.

In the case of MRE, the best procedure to apply the primer is to spray the primer dilution in a thin layer on the particles. By this treatment, the primer could be applied homogeneously on the particles while avoiding particle aggregates among the aligned chains.

Remarkable stiffening could be observed past a critical strain threshold that increases as the volume fraction of the particles decreases (>80 % deformation in the case of the 30 % volume fraction MREs). Beyond that critical strain threshold, strong bonds due to the primer application start to stiffen the composite material and seem to prevent debonding of the particles from the matrix.

**Acknowledgments** The authors wish to thank Alexandre Tanguy and Vincent de Greef at the Solid Mechanics Laboratory at Ecole Polytechnique for their contribution to the SEM images and the electronic devices, respectively.

### References

Böhm J (2001) Der Payneeffekt: Interpretation und Anwendung in einem neuen Materialgesetz für Elastomere. Dissertation, University of Erlangen  
 Bolzmacher C, Changeon G, Plaud V, Roselier S, Lozada J, Hafez M (2011) Tactile refreshable screen based on

- magneto-rheological fluids for map exploration and navigation tasks. *Proc SPIE Smart Sensors Actuators and MEMS V* Vol 8066. doi:10.1117/12.886982
- Carlson JD, Jolly MR (2000) MR fluid, foam and elastomer devices. *Mechatron* 10:555–569. doi:10.1016/S0957-4158(99)00064-1
- Coquelle E, Bossis G (2006) Mullins effect in elastomers filled with particles aligned by a magnetic field. *Int J Solid Struct* 43:7659–7672. doi:10.1016/j.ijsolstr.2006.03.020
- Coquelle E, Bossis G, Szabo D, Giulieri F (2006) Micromechanical analysis of an elastomer filled with particles organized in chain-like structure. *J Mater Sci* 41:5941–5953. doi:10.1007/s10853-006-0329-8
- Creton C, Hooker J, Shull KR (2001) Bulk and interfacial contributions to the debonding mechanisms of soft adhesives: extension to large strains. *Langmuir* 17:4948–4954. doi:10.1021/la010117g
- Dekkers MEJ, Heikens D (1983) The effect of interfacial adhesion on the tensile behavior of polystyrene-glass-bead composites. *J Appl Polym Sci* 28:3809–3815. doi:10.1002/app.1983.070281220
- Diani J, Fayolle B, Gilormini P (2009) A review on the Mullins effect. *Eur Polym J* 45:601–612. doi:10.1016/j.eurpolymj.2008.11.017
- Dorfmann A, Ogden RW (2004) A constitutive model for the Mullins effect with permanent set in particle-reinforced rubber. *Int J Solid Struct* 41:1855–1878. doi:10.1016/j.ijsolstr.2003.11.014
- Fan YC, Gong XL, Jiang WQ, Zhang W, Wei B, Li WH (2010) Effect of maleic anhydride on the damping property of magnetorheological elastomers. *Smart Mater Struct* 19:055015. doi:10.1088/0964-1726/19/5/055015
- Fu SY, Feng XQ, Lauke B, Mai YW (2008) Effects of particle size, particle/matrix interface adhesion and particle loading on mechanical properties of particulate-polymer composites. *Comp Part B* 39:933–961. doi:10.1016/j.compositesb.2008.01.002
- Geissler M, Xia Y (2004) Patterning: principles and some new developments. *Adv Mater* 16:1249–1269. doi:10.1002/adma.200400835
- Gent AN, Park B (1984) Failure processes in elastomers at or near a rigid spherical inclusion. *J Mater Sci* 19:1947–1956. doi:10.1007/BF00550265
- Habenicht G (2006) *Kleben*. Springer Heidelberg, Berlin
- Jansen Y, Karrer T, Borchers J (2010) MudPad: tactile feedback and haptic texture overlay for touch surfaces. In: *Proceedings of the ACM International Conference on Interactive Tabletops and Surfaces*. doi:10.1145/1936652.1936655
- Kallio M (2005) The elastic and damping properties of magnetorheological elastomers. Dissertation, VTT Technical Research Centre of Finland
- Leblanc JL (2002) Rubber-filler interactions and rheological properties in filled compounds. *Prog Polym Sci* 27:627–687. doi:10.1016/S0079-6700(01)00040-5
- Lee CH, Jang MG (2011) Virtual surface characteristics of a tactile display using magneto-rheological fluids. *Sens* 11:2845–2856. doi:10.3390/s110302845
- Léger L, Creton C (2008) Adhesion mechanisms at soft polymer interfaces. *Phil Trans R Soc A* 366:1425–1442. doi:10.1098/rsta.2007.2166
- Li W, Zhang X (2008) Research and applications of MR elastomers. *Recent Pat Mech Eng* 1:161–166. doi:10.2174/2212797610801030161
- Miehe C, Keck J (2000) Superimposed finite elastic-viscoelastic-plastoelastic stress response with damage in filled rubbery polymers. Experiments, modelling and algorithmic implementation. *J Mech Phys Solid* 48:323–365. doi:10.1016/S0022-5096(99)00017-4
- Mullins L, Tobin NR (1957) Theoretical model for the elastic behavior of filler-reinforced vulcanized rubbers. *Rubber Chem Technol* 30:555–571. doi:10.5254/1.3542705
- Payne AR (1962) The dynamic properties of carbon black-loaded natural rubber vulcanizates. Part I. *J Appl Polym Sci* 6:57–63. doi:10.1002/app.1962.070061906
- Peignot P, Rhodes K (2004) Choosing a silicone adhesive and treatment system. *Med Device Technol* 15:22–24
- Ramier J (2004) *Comportement mécanique d'élastomères chargés, Influence de l'adhésion charge-polymère, Influence de la morphologie*. Dissertation, University of Lyon
- Sgambelluri N, Scilingo EP, Rizzo R, Bicchi A (2008) A free-hand haptic interface based on magnetorheological fluids. *Springer Tracts Adv Robot* 45:155–178. doi:10.1007/978-3-540-79035-8\_8
- Vidal-Verdu F, Hafez M (2007) Graphical tactile displays for visually-impaired people. *IEEE Trans Syst Rehabil Eng* 15:119–130. doi:10.1109/TNSRE.2007.891375
- Wang MJ (1999) The role of filler networking in dynamic properties of filled rubber. *Rubber Chem Technol* 1999(72):430–448. doi:10.5254/1.3538812
- Wang Y, Hu Y, Chen L, Gong X, Jiang W, Zhang P, Chen Z (2006) Effects of rubber/magnetic particle interactions on the performance of magnetorheological elastomers. *Polym Test* 25:262–267. doi:10.1016/j.polymertesting.2005.10.002
- Yatsuyanagi F, Suzuki N, Ito M, Kaidou H (2001) Effects of secondary structure of fillers on the mechanical properties of silica filled rubber systems. *Polym* 42:9523–9529. doi:10.1016/S0032-3861(01)00472-4
- Zhang XZ, Gong XL, Zhang PQ, Li WH (2007) Existence of bound-rubber in magnetorheological elastomers and its influence on material properties. *Chin J Chem Phys* 20:173–179. doi:10.1360/cjcp2007.20(2).173.7